

## Van Hove scenario for $d$ -wave superconductivity in cuprates

D. M. Newns, C. C. Tsuei, and P. C. Pattnaik

IBM Thomas J. Watson Research Center, Yorktown Heights, New York, 10598

(Received 28 October 1994; revised manuscript received 30 June 1995)

The Van Hove scenario has so far been primarily based on the assumption of  $s$ -wave pairing as regards the treatment of superconducting properties. We investigate the assumption that pairing is  $d_{x^2-y^2}$  symmetry in an investigation of transition temperature, gap, and specific-heat jump at the BCS level of approximation. It is found that the effect of the Van Hove singularity on these properties is similar to, and at least as strong as, the effect in  $s$  wave. The  $d$ -wave version of the Van Hove scenario is found to be fully viable.

### I. INTRODUCTION

The idea of the Van Hove scenario<sup>1</sup> in its essence is that many of the special properties of the cuprate superconductors are attributable to the presence close to the Fermi level of *saddle points* in the band-structure energy surface. These are found to have strong implications in two-dimensional (2D) or nearly 2D electron systems such as the cuprate materials are known to be. Associated with the saddle points (SP's), which are flat regions of the energy dispersion, is the logarithmic (in two dimensions) singularity in the density of state<sup>1</sup> (DOS), known as the Van Hove singularity (VHS).

Three basic effects (at least) of the SP's on electronic properties have been detailed. First, the superconducting transition temperature is enhanced by having a DOS peak near the Fermi energy,<sup>1-3</sup> so that as the Fermi energy (experimentally, this can be controlled by doping) is swept through the VHS, the transition temperature goes through a maximum<sup>1-3</sup> at the point where the VHS and the Fermi energy coincide.

Secondly, there is a qualitative enhancement in the scattering between quasiparticles.<sup>1,4</sup> In a conventional metal, direct quasiparticle-quasiparticle scattering is almost completely suppressed, because it is nearly impossible to find significant phase space for a pair of quasiparticles to scatter into, given the thinness of the shell of thermally excited quasiparticles around the Fermi surface, relative to the Fermi energy  $E_F$ . But analysis shows<sup>1,4</sup> that when the VHS and  $E_F$  coincide, or the relative energy<sup>4</sup> of the VHS and  $E_F$  are within  $\sim$ temperature  $T$ , the phase space for scattering is much less restricted, leading to the "marginal-Fermi-liquid" (MFL) property<sup>1,4</sup> that lifetime broadening for quasiparticles is of order their energy measured from  $E_F$ .

The third effect<sup>1</sup> of having the VHS close to  $E_F$  is that for realistic models the Fermi surface (see Fig. 1) does not have a significant flat portion (note the area inside the surface differs from that outside by  $2 \times$  doping, building in the type of asymmetry seen in the figure and restricting any flat portion). This absence of flat portions inhibits "nesting" scattering which, in the metallic phase, enhances antiferromagnetic spin-density-wave (SDW) or charge-density-wave (CDW) instabilities. These are the strongest competing instabilities for superconductivity.

Experimentally, the saddle points near  $E_F$  are indeed seen directly in angle-resolved photoemission spectroscopy experiments<sup>5,6</sup> on maximal- $T_c$  materials. Analysis of specific-heat-jump data<sup>1</sup> supports the presence of the VHS in the DOS. The MFL behavior seems to underlie transport anomalies such as the linear resistivity<sup>1,4</sup> and  $T$ -independent thermopower,<sup>4</sup> which also are associated with the vicinity of maximal  $T_c$ . And the correlation length for the SDW instability (expected to dominate CDW for repulsive interactions) is short, of order one lattice spacing,<sup>7</sup> near maximal  $T_c$ . This experimental picture is entirely consistent with the Van Hove scenario.

However, while the superconducting aspects of the scenario (transition temperature,<sup>1-3</sup> isotope shift,<sup>1</sup> specific-heat jump<sup>1</sup>...) have been worked out on the basis of  $s$ -wave pairing, recent experiments<sup>8-11</sup> seem to increasingly favor  $d$ -wave, in particular  $d_{x^2-y^2}$ , pairing. For example, measurements<sup>8</sup> of the NMR  $1/T_1$  below  $T_c$ , the low-temperature magnetic penetration depth,<sup>9</sup> and recently measurements of the phase of the order parameter,<sup>10,11</sup> seem to pose insurmountable problems for an  $s$ -wave interpretation.

Is the Van Hove scenario consistent with  $d$ -wave pairing symmetry? This paper revisits the Van Hove issue from a  $d$ -wave point of view, within a simplistic BCS-type level of approximation. We calculate the effects of the VHS on a few

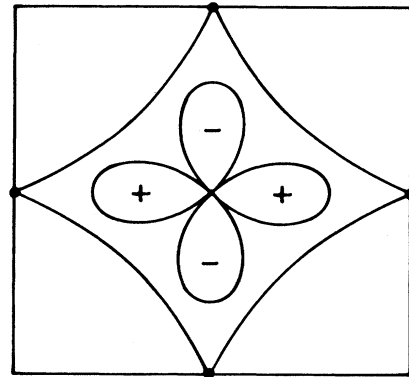


FIG. 1. Idealized Fermi surface in Van Hove scenario, showing saddle points (full circles) and lobes of  $d_{x^2-y^2}$  order parameter.

key properties, transition temperature, gap, and specific-heat jump, and find that this is extremely strong, just as in  $s$  wave. The reason is easily seen from Fig. 1. The lobes of the  $d_{x^2-y^2}$  order parameter point towards the high-DOS regions around the SP's. The zeroes of the order parameter lie in low-DOS regions away from the SP's. Hence the gap equation is dominated by what is happening to the SP's, which act to stabilize the  $d_{x^2-y^2}$  order parameter, and is not much affected by the other parts of the Fermi surface. Destabilization of  $s$ -wave pairing is caused by the presence of the large on-site Coulomb repulsion  $U$ , which is fatal in the  $s$ -wave channel, but which drops out of the  $d$ -wave gap equation.

In an earlier study of pairing induced by spin fluctuations, Radtke *et al.*<sup>12</sup> came to a negative conclusion about the significance of the Van Hove singularity. In a recent paper, Dagotto *et al.*,<sup>13</sup> in a BCS calculation, come independently to similar, though not identical, conclusions to the present work.

The driving force for  $d$ -wave pairing is an interaction of the type which is attractive for electrons on nearest-neighbor sites. Perhaps the most plausible candidate is the antiferromagnetic superexchange  $J$ , which is known to be a huge effect ( $J \sim 120$  meV) in the undoped insulator. We have earlier drawn attention to the requirement<sup>1</sup> for an interaction  $J$  in order to explain the nearly  $T$ -independent static long-wavelength susceptibility. The short-wavelength susceptibility (coming for example into<sup>14,15</sup> the NMR  $1/T_1$ ) is also strongly effected by  $J$ . Note that these effects are opposite because of the dispersion of  $J$  [see below (10) in the following], the uniform susceptibility is reduced<sup>1</sup> and rendered  $T$  independent by  $J$ , while the short-wavelength one is enhanced and acquires a broad peak as a function of wave vector.<sup>14,15</sup>

Recently one of us and co-workers have implemented Monte Carlo simulations<sup>16</sup> on the  $tt'$  model in the presence of the repulsive on-site interaction  $U$ . We found that  $d_{x^2-y^2}$  pairing was present, but only when the Fermi level lay in the close vicinity of the VHS. This supports not only the Van Hove scenario but also an essentially electronic origin of the pairing interaction.

However, we also consider the possibility that the interaction may be charge mediated, in particular phononic, in type. For this case we calculate the isotope shift which qualitatively resembles (and even improves with regard to the comparison with data) the  $s$ -wave result.

## II. THEORETICAL APPROACH

Before considering in detail the implications of  $d$ -wave pairing for the Van Hove scenario, it is useful to discuss briefly the relevant normal-state effects of the electronic interactions. Let us start by considering self-energy effects.

The superexchange interaction  $J$  is a nonretarded interaction; however, its  $k$ -dependence results in a contribution to the effective mass to  $O(J)$ . To specify this contribution to  $O(J)$ , consider the decomposition of  $J$  into separable terms [carried out in Eq. (11) below]. Only the  $\gamma$  term contributes to the self-energy, which has the  $k$  dependence of  $\gamma_k$ , and thus merely renormalizes the  $t$  term in the Hamiltonian (5) by an amount of order  $J$ . This renormalization of  $t$  can be absorbed into the parametrization of the model.

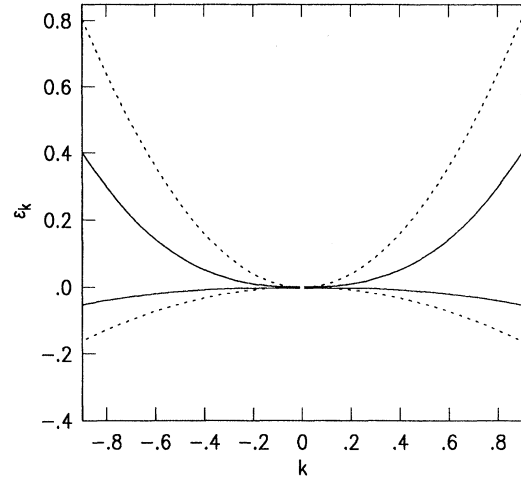


FIG. 2. Dashed curve: dispersion for hyperbolic model  $\varepsilon_k = k_x^2 - k_y^2/5$  plotted vs  $k (=k_x \text{ or } k_y)$ . Full curve: dispersion from maximum of Eq. (2) with  $\alpha = 1.0$ .

The more important effect which we wish to discuss arises from the interaction responsible for the anomalous (linear in energy from the Fermi surface) lifetime broadening of the quasiparticles in cuprates. In the Van Hove scenario, this arises naturally from the short-range screened interelectronic interaction plus the anomalous phase space around the VHS, and is found on calculating the imaginary part of the self-energy to second order in the interaction. As discussed in Appendix A, we can most simply model the imaginary part  $B(\omega)$  of the self-energy by the ansatz  $\text{Im}\Sigma = B(\omega) = \alpha|\omega|$ , where  $\alpha$  parametrizes the strength of the interaction and is of order 0.5. The real part of the self-energy  $A(\omega) = \text{Re}\Sigma = (-\alpha\omega/\pi)\ln|(D^2 - \omega^2)/\omega^2|$ , is then obtained by Hilbert transforming the imaginary part.

The single-particle Green's function

$$G_k(\omega) = \frac{1}{\omega - \varepsilon_k - A(\omega) + iB(\omega)} \quad (1)$$

leads to the spectral density

$$S_k(\omega) = \frac{\pi^{-1}B(\omega)}{[\omega - \varepsilon_k - A(\omega)]^2 + B(\omega)^2}. \quad (2)$$

The true maximum in (2), approximately given by

$$\tilde{\varepsilon}_k \approx \varepsilon_k / [1 + (2\alpha/\pi)\ln|D/\varepsilon_k|],$$

is plotted as a function of  $k$  in Fig. 2 for the hyperbolic model

$$\varepsilon_k = k_x^2 - \frac{k_y^2}{5}. \quad (3)$$

We see from Fig. 2 that the renormalized dispersion is flatter at low energies, relative to the pure hyperbola, essentially due to the divergence of the effective mass at low energies. Note that this flattened dispersion strongly resembles the ‘‘extended saddle point’’ type of dispersion seen in experimental data such as angle-resolved photoemission.<sup>5</sup>

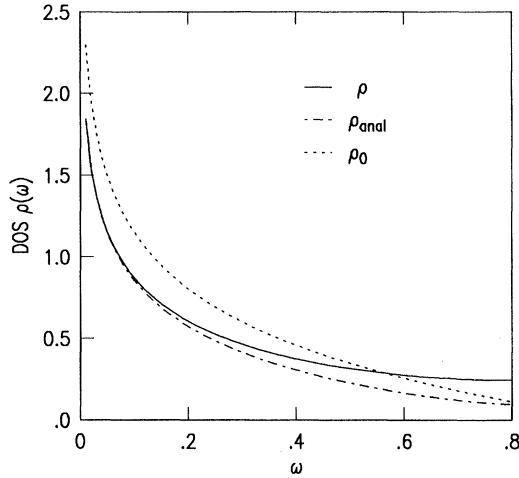


FIG. 3. Densities of states, dashed curve simple hyperbolic dispersion  $\varepsilon_k = k_x k_y$ , full curve Eq. (4), with  $\alpha = 0.5$ , dot-dash curve analytic approximation (A5) with same value of  $\alpha$ .

The renormalized density of states

$$\rho(\omega) = \frac{1}{\pi N} \sum_k S_k(\omega) \quad (4)$$

is also of interest and is illustrated in Fig. 3 for the simplest dispersion  $\varepsilon_k = k_x k_y$ . Because of the mass enhancement at low  $\varepsilon_k$ , illustrated in Fig. 2, the density-of-states peak is seen in Fig. 3 to be narrower than the pure Van Hove logarithmic form. However, the peak is not higher than in the logarithmic case. The feature that the peak is not higher, though it is narrower, than in the noninteracting case, may be attributed to the  $z$ -factor effect: the DOS as defined is multiplied by a  $z$  factor approximately given by  $1/[1 + (2\alpha/\pi)\ln|D/\omega|]$ , which cancels the DOS enhancement. It is sometimes appropriate to define a quasiparticle density of states  $\tilde{\rho} = \rho/z$ , derived from giving the quasiparticle approximation to the spectral density peak in (1) unit weight. In the present problem the quasiparticle density of states would have a peak that is both higher and narrower than the noninteracting DOS peak.

The effective-mass corrections in superconductivity are a more complex issue: the  $z$  factor enters explicitly, and the vertex correction may not necessarily be neglected. In the well-studied case of phonon-mediated pairing, in a flat region of the density of states, the vertex correction is negligible (Migdal theorem) if the phonon frequencies are much lower than any band-structure energy scale near the Fermi energy. In the Eliashberg approximation the  $k$  dependence is neglected, and there are constant mass enhancement and  $z$  factors, defined in terms of the dimensionless coupling strength  $\lambda$ , as  $m^*/m = 1 + \lambda$ ,  $z = 1/(1 + \lambda)$ . Since two single-particle propagators are involved in pairing, the  $z$  factor comes in twice. The factor  $z^2 \tilde{\rho} = z\rho$  is then the density of states entering pairing in this approach. The effect of the interactions is to reduce the density of states by the factor  $z$  relative to the noninteracting one.

A contrary paradigm to the phonon pairing one is found in the higher- $l$ -wave pairing model for heavy fermion systems.

In heavy fermion systems, turning on the interaction, which is an on-site Coulomb repulsion, results in the formation of spins on the rare-earth sites which turn over slowly due to the orthogonality catastrophe (Kondo effect) and thus result in extremely heavy  $f$  bands. The pairing interaction is a Ruderman-Kittel-Kasuya-Yosida interaction  $K$ , which couples to the  $f$  bands. In the analysis provided by the slave-boson mean-field approach, the heavy mass is derived from self-consistently generated (small) mean-field values of the  $f$ - $d$  hopping integrals.  $z$  factors only come in through  $f$ - $d$  hopping processes. Since  $K$  only couples to  $f$ , there are no  $z$  factors. Hence the DOS which enters at the mean-level is  $\tilde{\rho}$ . In this case, the effect of the interaction is to enhance the DOS appearing in the pairing formula.

The present problem, in which the interaction is taken to be the superexchange  $J$ , lacks a Migdal theorem. There is no frequency dependence of  $J$ . The interaction responsible for the marginal-Fermi-liquid properties exists only due to the Van Hove singularity itself, and cannot therefore be supposed to contain any different energy scale from the band-structure feature, also the VHS. Hence there is no *a priori* reason to believe in a Migdal theorem in this context. The DOS entering into the pairing problem may then not necessarily be  $z^2 \tilde{\rho}$ , as in the Migdal case, in fact a study of phonon-mediated pairing including vertex corrections<sup>17</sup> found a tendency for the  $z$  factor to revert towards unity. Without a careful calculation at the vertex correction level, we cannot be sure how the  $z$  factors do enter in the present case. Note that purely formal attempts to treat the problem, say on the basis of the Hubbard model, require going up to order  $U$ ,<sup>4</sup> which has not yet been attempted.

The conclusion that may be drawn is that in a treatment of pairing the DOS singularity (VHS) may be narrowed due to the interaction effects, but we find no reason to think it broadened. There may be some  $z$ -factor effects, which can be to a certain extent absorbed into the definition of  $J$ . By proceeding using the BCS theory, we have no reason to doubt that the effects of the VHS may be underestimated, while the value of  $J$  needed to achieve a given pairing strength may be underestimated (if the ultimate many-body theory is phonon-like) or overestimated (if it is heavy fermion like). Hence the following BCS investigation should give a feeling for the importance of the VHS for  $d$ -wave pairing, but would be less reliable in indicating a correct value for the interaction  $J$ .

### III. MODEL

We wish to discuss models which are compatible with the Van Hove scenario. The requirement is that when the saddle points in the band structure  $\varepsilon_k$  surface (=the Van Hove singularities in the density of states) lie near the Fermi surface, the system be hole doped. In a single-band model this ensures that the band will be less than half-filled, and thus that the Fermi surface be qualitatively of the asymmetric (with regard to the electron and hole regions) type<sup>1</sup> illustrated in Fig. 1.

The simplest such model on a single orbital per site square lattice is the  $tt'$  model

$$\mathcal{H} = -t \sum_{\langle ij \rangle, \sigma} (c_{i\sigma}^+ c_{j\sigma} + \text{H.c.}) + t' \sum_{\langle\langle ij \rangle\rangle, \sigma} (c_{i\sigma}^+ c_{j\sigma} + \text{H.c.}). \quad (5)$$

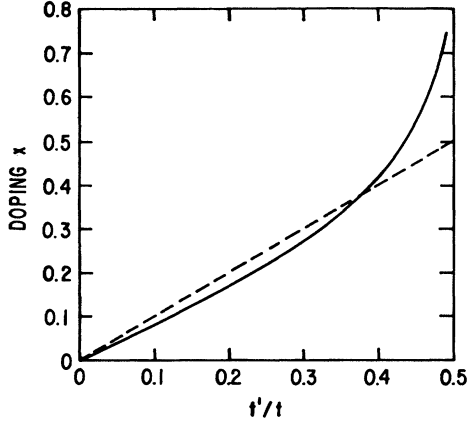


FIG. 4. Full curve: variation of doping  $x$  required to keep the saddle points at the Fermi level as  $t'$  is turned on in  $tt'$  model. Dashed curve: line  $x = t'/t$ .

Here  $\langle \rangle$  implies nearest neighbors, and  $\langle\langle \rangle\rangle$  implies next-nearest neighbors. We are interested in the regime  $0 < t' < 0.5t$ , in which the saddle points lie at  $(\pi, 0)$  and  $(0, \pi)$  and at energy  $-4t'$ , as can be seen from the dispersion of the energy band  $\varepsilon_k$

$$\varepsilon_k = -2t(\cos k_x + \cos k_y) + 4t' \cos k_x \cos k_y. \quad (6)$$

At  $t' = 0$ , the saddle point is at the band center, the Fermi level coincides with it for the half-filled (zero doping) case. As  $t'$  is increased, the doping required to keep the saddle point (SP) at  $E_F$  also increases, the plot of filling vs  $t'$  is shown in Fig. 4; up to a doping of nearly 0.4, the doping and the corresponding value of  $t'/t$  are approximately equal.

Near the saddle points, the energy surface is approximately hyperbolic, for example around  $(\pi, 0)$  (6) may be expanded as

$$\varepsilon_k = -4t' - k_x^2[t - 2t'] + k_y^2[t + 2t']. \quad (7)$$

The surface (7) is seen to be downwardly convex in the  $k_x$  direction, with a heavy mass  $m_d \sim 1/(t - 2t')$ , and to be upwardly convex in the  $k_y$  direction, with a light mass  $m_u \sim 1/(t + 2t')$ . In the limit  $t'/t \rightarrow 0.5$ , the mass ratio  $m_d/m_u = (t + 2t')/(t - 2t')$  actually diverges, a form of the extended saddle point<sup>5</sup> situation. At the other saddle point,  $(0, \pi)$ , the  $k_x$  and  $k_y$  directions in (7) are interchanged.

An example of the Fermi surface is shown in Fig. 1; near the saddle point the Fermi surface forms the asymptotes of the hyperbolas in (7), notice that they are nonrectangular. This is seen in Eq. (7) to be again due to the presence of the interaction  $t'$ , in whose absence the energy surface is represented by the rectangular hyperbolic form  $t(k_y^2 - k_x^2)$ .

The nonrectangularity of the hyperbolic surfaces around the two saddle points is in qualitative agreement with angle-resolved photoemission, where the mass ratio is seen clearly to be very large.<sup>5</sup> It is believed in the Van Hove scenario to have important physical implications for electron-hole instabilities in the SDW or CDW channels. For these electron-hole instabilities to diverge most strongly at the wave vector  $(\pi, \pi)$  in the metallic phase, it is necessary to have the two

saddle points mapping onto each other by a dispersive transformation in  $k$  space (nesting). The mapping occurs in the idealized  $t' = 0$ , half-filled case, leading to very strong SDW and CDW instabilities. But in the case  $t' \neq 0$ , even with the SP's at  $E_F$ , the mapping (nesting) is greatly reduced. This allows the superconducting instability, which is not weakened by eliminating nesting (to which it is insensitive), but is strongly enhanced by the density of states peak associated with the Van Hove singularity lying at the Fermi surface, to become the leading instability. Pairing in cuprate superconductors is believed to benefit from the strong DOS peak due to the VHS, and the absence of competing instabilities.

We wish to consider interactions favoring  $d_{x^2-y^2}$  pairing. These are of the type tending to stabilize a configuration of two electrons sitting on nearest-neighbor sites, and an attractive nearest-neighbor interaction is the simplest to assume. A nearest-neighbor antiferromagnetic exchange interaction is the most natural assumption and takes the form

$$\mathcal{H}_{\text{int}} = J_0 \sum_{\langle ij \rangle} \mathbf{S}_i \cdot \mathbf{S}_j, \quad (8)$$

where  $S = 1/2$ ,  $J_0 > 0$ , and the sum is over all nearest-neighbor bonds. A similar effect can be produced by an interaction in the charge channel, e.g.,

$$\mathcal{H}_{\text{int}} = V \sum_{\langle ij \rangle \sigma \sigma'} n_{i\sigma} n_{j\sigma'}, \quad (9)$$

where  $V < 0$ . We adopt the notation (8) in the following. The resulting BCS gap equation is

$$\Delta_k = \sum_{k'} J(k - k') \frac{\Delta_{k'}}{2E_{k'}} \tanh\left(\frac{E_{k'}}{2T}\right), \quad (10)$$

where  $J(q) = 2J(\cos q_x + \cos q_y)$  is derived from the Fourier transformation of (8),  $E_k^2 = (\varepsilon_k - \mu)^2 + \Delta_k^2$ , and  $J = 3J_0/4$ .

Equation (10) is exactly soluble<sup>18</sup> for this form of  $J$ , because of its separability:

$$J(k - k') = J \eta_k \eta_{k'} + J \gamma_k \gamma_{k'} + \text{odd terms}, \quad (11)$$

where  $\eta_k = (\cos k_x - \cos k_y)$  and  $\gamma_k = (\cos k_x + \cos k_y)$  are the  $d_{x^2-y^2}$  and extended- $s$  form factors. The odd solutions have nodes through the high-DOS saddle-point regions of  $k$  space, and are not expected to play a role in the present context.

The relative stability of the extended- $s$  and  $d_{x^2-y^2}$  solutions has been discussed extensively<sup>18</sup> by Wheatley and Xiang, who found that only the  $d_{x^2-y^2}$  solution is stable in the region of the phase diagram of interest in the present paper. The  $d_{x^2-y^2}$  gap equation is given by

$$1 = J \sum_k \frac{\eta_k^2}{2E_k} \tanh\left(\frac{E_k}{2T}\right), \quad (12)$$

where  $\Delta_k = \Delta \eta_k$  defines the gap parameter  $\Delta$ . The gap varies from a maximum of  $2\Delta$  at the  $(\pi, 0)$  SP to a minimum of  $-2\Delta$  at the other SP  $(0, \pi)$ .

In Fig. 5 we plot both the transition temperature and the zero- $T$  gap as a function of the position of the Fermi level with respect to the Van Hove singularity, equivalently the doping. It is seen that the ratio of  $2 \times$  maximum gap to transition temperature is about 4.2 (slightly higher than the

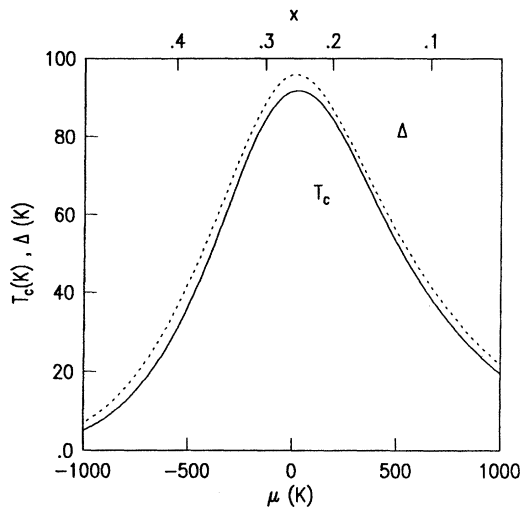


FIG. 5. Plot of  $T_c$  and gap parameter  $\Delta$  in  $tt'$  model, for  $d_{x^2-y^2}$  pairing, vs energy  $\mu$  of the Fermi level relative to the VHS (lower scale) and doping  $x$  (upper scale). Parameters  $t=2500$  K,  $t'=715$  K,  $J=1200$  K, the VHS being then located at  $-2860$  K.

$s$ -wave BCS ratio of 3.5), and that both the gap and transition temperature peak extremely strongly around the point where the Fermi level lies at the saddle point. It is clear that, at least in BCS theory, strong  $d$ -wave pairing, as  $s$ -wave pairing, is a phenomenon mainly confined to the vicinity of the Van Hove singularity. This singularity survives in the presence of the marginal-Fermi-liquid lifetime broadening (see Sec. II), so that our conclusions about the Van Hove induced peak in  $T_c$  should remain valid in a more general treatment.

In Fig. 6 we illustrate the zero- $T$  density of states. The linear behavior at low energies is characteristic of  $d$ -wave symmetry in two dimensions,<sup>19</sup> and contrasts with the  $s$ -wave situation where there are no states in the gap; the states in the  $d$ -wave case come from the part of the Fermi

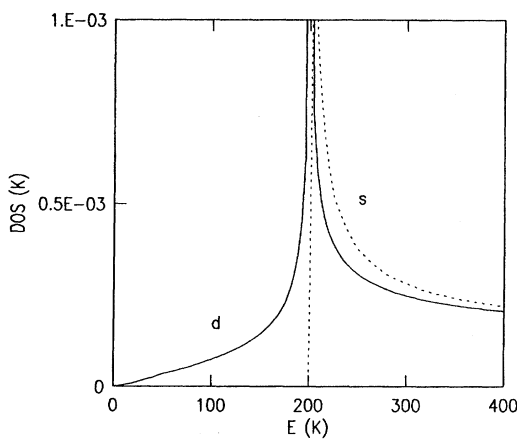


FIG. 6. Density of states at  $T=0$  for  $s$ - and  $d$ -wave pairing compared. The band structure parameters are as in the previous figure, with the Fermi level located at the VHS. In the  $d$ -wave case the gap parameter is  $\Delta=100$  K, while in the  $s$ -wave case the gap is 200 K.

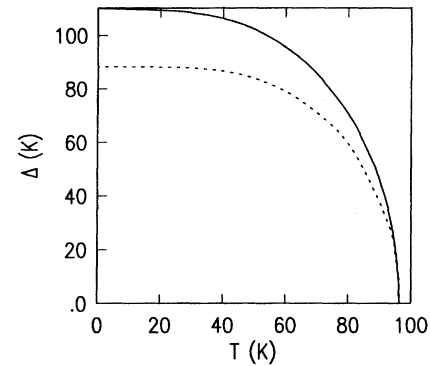


FIG. 7. Full curve, plot of gap parameter  $\Delta$  vs temperature in the  $d$ -wave case, parameters correspond to “extended” saddle point,  $t=2500$  K,  $t'=1125$  K,  $J=1100$  K. Dashed curve, BCS gap/2 for on-site attraction  $W=2140$  K, with cutoff frequency 700 K, other parameters the same.

surface around the node in the gap function (see Fig. 1). The peak at the maximum gap,  $2\Delta$ , is similar to the well-known peak in the  $s$ -wave BCS density of states, but when approached from above it is seen to be a weaker singularity in the  $d$ -wave case.

A gap vs temperature plot is illustrated in Fig. 7, obtained by solving the gap equation (12). The case selected is the extended SP situation with a ratio  $m_d/m_u=19$ . Comparison with conventional BCS  $s$ -wave shows the somewhat greater maximum gap in the  $d$ -wave case for the same transition temperature, otherwise the curve is unremarkable.

To complete this section, we imagine that the interaction was in fact of the charge-coupled type (9), mediated by phonons. In that case, there would be an isotope shift,<sup>1,2</sup> and in Fig. 8 we illustrate  $T_c$  and isotope shift  $\alpha$  as a function of doping. It is seen that as in the  $s$ -wave case, there is a pronounced minimum in the isotope shift at the place where the transition temperature has a maximum. The minimum  $\alpha$  is

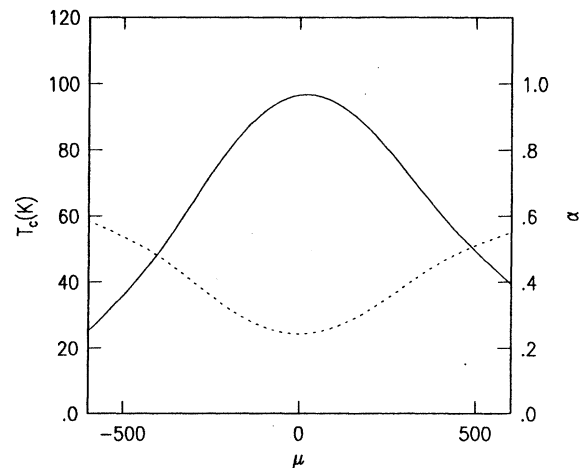


FIG. 8.  $T_c$  and isotope shift  $\alpha$  plotted vs energy of the Fermi level relative to the VHS, for the case of an interaction like (9) mediated by phonons. Parameters  $t=2500$  K,  $t'=715$  K,  $V=1700$  K, phonon cutoff  $\omega_c=700$  K.

somewhat lower than in the  $s$ -wave case (in better agreement with experimental data); the isotope shift minimum may be further lowered by anharmonic and  $z$  factor (see Sec. II) effects.

#### IV. SPECIFIC HEAT

One of the key features in the Van Hove scenario, established in previous work,<sup>1,2</sup> was the peak in the specific-heat jump occurring when the doping corresponded to the maximum transition temperature. The underlying reason was that the DOS peak at  $E_F$  is maximum at that point, which is reflected in the specific-heat jump, as calculated both in the BCS and Eliashberg<sup>1</sup> formalisms. There is a lot of experimental support<sup>1</sup> for this correlation between the maximum transition temperature and the maximum in the specific-heat jump, providing support for the Van Hove scenario.

In this section we address two issues arising from this previously established correlation. The first is to establish that the specific-heat jump also correlates with maximum  $T_c$  in  $d$ -wave symmetry. Secondly we address the issue of the specific-heat behavior in the normal state at temperatures well above the transition temperature, our motivation being that measurements<sup>20</sup> do not show any sign of the Van Hove peak in the DOS in the normal state, giving rise to criticism of the entire Van Hove scenario.

To anticipate our conclusion, we find that the specific-heat jump has a pronounced maximum, in pairing of  $d_{x^2-y^2}$  symmetry, at the doping corresponding to maximum  $T_c$ , analogous to the  $s$ -wave case. However no significant structure is found in the normal-state specific heat. These results are in agreement with experiment and support the scenario.

We shall stick to the BCS level of approximation in this paper, and follow the method of Fetter and Walecka<sup>21</sup> in calculating the specific-heat jump. The free-energy difference between normal and superconducting states is first written as a coupling constant integration

$$\Omega_s - \Omega_n = \int_0^1 \frac{d\lambda}{\lambda} \langle \lambda \mathcal{H}_{\text{int}} \rangle, \quad (13)$$

where  $\lambda$  is a coupling constant multiplying  $J$ . Using (8) this may be rewritten

$$\Omega_s - \Omega_n = - \int_0^J \frac{dJ}{J^2} \Delta^2,$$

or

$$\Omega_s - \Omega_n = - \frac{\Delta^4}{2} X(T), \quad (14)$$

where

$$X(T) = \sum_k \frac{\eta_k^4}{4\xi_k^3} \left[ \tanh\left(\frac{\xi_k}{2T}\right) - \frac{\xi_k}{2T} \text{sech}^2\left(\frac{\xi_k}{2T}\right) \right], \quad (15)$$

and  $\zeta_k = \varepsilon_k - \mu$ .

Using the gap equation (12), which is expanded for  $\Delta$  small and  $T$  close to  $T_c$ , (14) can be expressed as an expansion in  $T_c - T$ . Differentiating twice, we obtain the specific-heat jump

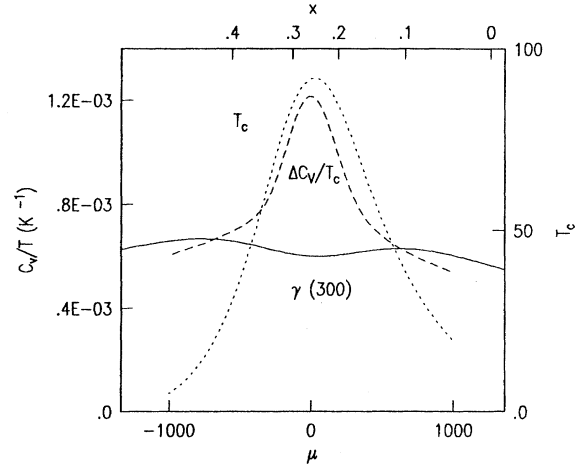


FIG. 9. Specific-heat jump  $\Delta C_v$  (dashed curve) in  $tt'$  model, for  $d_{x^2-y^2}$  pairing, vs energy of the Fermi level relative to the VHS (lower scale) and doping (upper scale). Parameters  $t=2500$  K,  $t'=715$  K,  $J=1200$  K. Also illustrated are transition temperature (dotted curve, right-hand scale) and normal-state specific-heat coefficient  $\gamma$  at 300 K (full curve).

$$\Delta C_v = \frac{k_B^2 Y^2(T_c)}{T_c^3 X(T_c)}, \quad (16)$$

where

$$Y(T) = \frac{1}{4} \sum_k \eta_k^2 \text{sech}^2\left(\frac{\xi_k}{2T}\right). \quad (17)$$

We may also calculate the normal-state electronic specific heat above  $T_c$ ,

$$C_v(T) = \frac{1}{2T^2} \sum_k \xi_k^2 \text{sech}^2\left(\frac{\xi_k}{2T}\right). \quad (18)$$

In Fig. 9 we illustrate the variation of  $T_c$ , specific-heat jump, and normal-state specific heat at 300 K, as a function of Fermi level relative to the VHS. We see that the specific-heat jump has a sharp maximum just at the place where the transition temperature peaks, as in the  $s$ -wave case. However the normal-state specific-heat jump does not peak at this point—due to the  $\xi_k^2$  factor in (18), there is instead a weak minimum. Experimental data<sup>20</sup> given in Fig. 10 are seen to have a close qualitative resemblance to the results of Fig. 9. Note that in the experimental figure doping goes to the right (somewhat qualitatively in terms of the oxygen concentration), while in Fig. 9 it goes to the left. In both figures the peak in transition temperature is associated with a narrower peak in the specific-heat jump, but a rather featureless normal-state specific heat.

A more quantitative calculation attempting to reproduce the data is limited by (a) our restriction to a one-band model, (b) the difficulty in reproducing the complicated extended saddle-point feature seen in the 123 material experimentally, and (c) neglect of the renormalization effects reproduced in the Eliashberg treatment. In Fig. 11 we do, however, present a semiquantitative attempt to reproduce the data, using pa-

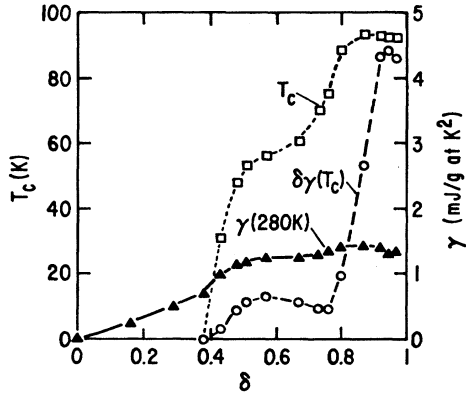


FIG. 10. Specific-heat jump  $\Delta C_v$  (dashed curve), transition temperature (dotted curve, left-hand scale) and normal-state specific-heat coefficient  $\gamma$  at 280 K (full curve), for  $\text{YBa}_2\text{Cu}_3\text{O}_{6+\delta}$  plotted vs  $\delta$ .

rameters partly reproducing the extended saddle-point situation (but not as effectively as done in Ref. 22). The main discrepancy from the experiment<sup>20</sup> is that the latter has about a factor of 2 higher specific heat. While this might be due to our choice of mass being too low, it is also possible that the  $\gamma$  value in the real material is raised by the contribution of multiple bands, while the specific-heat jump is enhanced by mass enhancement effects (Sec. II). The broad features of the experiment are reproduced, however.

## V. CONCLUSION

The BCS calculations in the present paper suggest that the  $d$ -wave version of the Van Hove scenario is as compelling as the earlier  $s$ -wave version. Key properties such as transition

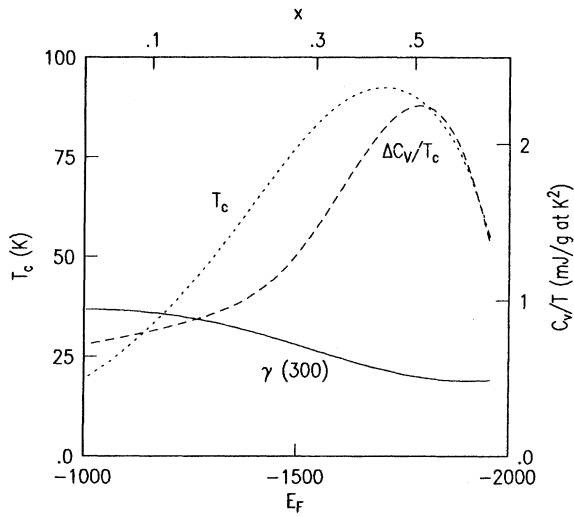


FIG. 11. Specific-heat jump  $\Delta C_v$  (dashed curve) in  $tt'$  model, for  $d_{x^2-y^2}$  pairing, vs energy of the Fermi level (lower scale) and doping (upper scale). Parameters  $t=1000$  K,  $t'=450$  K,  $J=720$  K. Also illustrated are transition temperature (dotted curve—left-hand scale) and normal-state specific-heat coefficient  $\gamma$  at 300 K (full curve).

temperature, gap, and specific-heat jump are dominated by the saddle points just as in the  $s$ -wave case. The phase space effects underlying this  $T_c$  enhancement should survive the introduction of a marginal Fermi liquid-type lifetime broadening, as demonstrated from a modelistic standpoint in Sec. II and the Appendix. The interaction we have assumed to drive the pairing is a nearest-neighbor attraction, most probably an antiferromagnetic exchange interaction. This interaction is also important in generating the  $T$ -independent bulk susceptibility, and in generating a broad peak in the magnetic  $S(q)$  at  $(\pi, \pi)$ , which is measured directly in neutron scattering and indirectly in NMR experiments. In this case the isotope shift is zero, however, posing a problem for the observed doping dependence of the isotope shift. In the case where the nearest-neighbor attractive interaction is phononic, the behavior of the isotope shift (minimum where the transition temperature is maximum) is the same as in the  $s$ -wave case.

The exchange interaction within the single-band model has a direct origin as a superexchange interaction from transforming away the oxygen bands, as in the  $tJ$  model. However, even in the single-band Hubbard model an exchange interaction of order  $t^2/U$  is present, and the exchange concept can be extended to smaller  $U$  by invoking perturbation theory in  $U$  which also generates exchange-type diagrams, starting at order  $U^2$ . Experimentally, measurements of  $J_0$  in the insulating phase suggest values<sup>23</sup> on the order of 120 meV.

Converting  $J$  values quantitatively into  $T_c$  values for cuprates is not possible using the BCS approximation because the vertex corrections, arising as a result of higher-order scattering in the repulsive Coulomb interaction  $U$  are ignored, as discussed in Sec. II.

In a quantum Monte Carlo study of the two-dimensional  $tt'$  Hubbard model some of the present authors and co-workers<sup>16</sup> found strong evidence for  $d_{x^2-y^2}$  symmetry pairing in the range of interaction strengths  $0.5t < U < 3t$ , when the Fermi level lies close to the energy of the saddle points, consistent with the Van Hove scenario. This purely electronic pairing effect is probably of exchange origin. By extracting a  $J$  value in a manner making allowance for  $z$ -factor effects, it was possible to estimate an approximate value of  $T_c$ , which at  $U=3t$  was found to be approximately 40 K.

An adequate *ab initio* investigation of the possible phononic contribution to  $d$ -wave pairing is so far not available. We can only briefly comment here on probabilities based on conceptually simple models. The breathing-type modes of in-plane oxygens (the result should also apply to “apex” oxygens), in which the oxygen motion lies along the bond joining it to its copper neighbors, tend to favor configurations in which a pair is localized on a site rather than in a bond, and thus favor  $s$ -wave pairing. On the other hand, in a buckled configuration of the “in-plane” oxygens, where these lie somewhat out of plane, motion of the oxygens normal to the plane promotes localization of electrons at opposite ends of a Cu-Cu bond, and thus should favor  $d$ -wave pairing. The degree of buckling is also strongly coupled to the electronic structure of the saddle points,<sup>24</sup> and in particular to their “extended” character. It remains for a detailed

calculation to investigate the possible consequences for pairing of this type of buckling-unbuckling motion of the “in-plane” oxygens.

At the present time the nearest-neighbor antiferromagnetic exchange supported by the VHS seems likely to underlie the pairing, which links up the Van Hove and the magnetic scenarios, without the implausibility of assuming that maximal  $T_c$  cuprates are on the verge of an antiferromagnetic instability. However, a synergic interaction involving, for example, the buckling-unbuckling motion of the planar oxygens, together with the antiferromagnetic exchange, may be significant, enabling retention of the standard Van Hove explanation of the anomalous isotope shift.

*Note added in proof:* Recently T. Hotta (private communication), has derived similar results to those of Sec. II in a fully  $k$ -dependent manner. In a renormalization group calculation, I. Ye. Dzyaloshinskii (private communication) has examined mass enhancement effects beyond perturbation theory, with interesting results including a non-Fermi liquid phase.

## APPENDIX

Misgivings are sometimes expressed as to whether the Van Hove density of states singularity, which plays a key role for superconductivity, survives the presence of lifetime broadening of the quasiparticles. To investigate this, we may start from a general definition of the density of states  $\rho(\omega)$

$$\begin{aligned}\rho(\omega) &= \frac{1}{\pi N} \sum_k \text{Im } G(k, \omega) \\ &= \frac{1}{\pi N} \sum_k \frac{|\text{Im } \Sigma(k, \omega)|}{[\omega - \varepsilon_k - \text{Re } \Sigma(k, \omega)]^2 + [\text{Im } \Sigma(k, \omega)]^2}.\end{aligned}\quad (\text{A1})$$

In the case of quasiparticle scattering around a Van Hove singularity, the lifetime broadening has been shown analytically

and numerically<sup>4</sup> to have an anomalous marginal Fermi liquid behavior, in which the on-shell lifetime broadening takes the form (assuming  $E_F = E_{\text{VHS}}$ )

$$\text{Im } \Sigma(k, \varepsilon_k) \sim \alpha \varepsilon_k. \quad (\text{A2})$$

The lifetime broadening is proportional to the quasiparticle energy measured from the Fermi level, instead of its square as in a normal Fermi liquid. The quantity  $\alpha$  is of order 1/2. This MFL-enhanced lifetime broadening is the cause of the concern as to the survival of the Van Hove singularity.

With the ansatz  $\text{Im } \Sigma(k, \omega) = \alpha |\omega| = B(\omega)$ , which extends the on-shell result (A2), an analytically tractable treatment of the effect of lifetime broadening on the DOS can be implemented. The real part of the self-energy, obtained from the Hilbert transform of  $B$ , is  $A(\omega) = -(\alpha/\pi)\omega \ln|(D^2 - \omega^2)/\omega^2|$ .

The normal-state DOS (A1) at a single saddle point with dispersion  $\varepsilon_k = k_x k_y$  takes the form

$$\rho(\omega) = \frac{1}{2D\pi} \int_0^{k_c} dk_x \int_{-k_c}^{k_c} dk_y \frac{B(\omega)}{[\omega - k_x k_y - A(\omega)]^2 + B(\omega)^2}, \quad (\text{A3})$$

here  $k_c$  is related to the bandwidth cutoff  $D$  by  $k_c^2 = D$ .

In terms of spectral density

$$\rho(\omega) = \frac{1}{\pi} \int_{-D}^D d\varepsilon \frac{\rho_0(\varepsilon) B(\omega)}{[\omega - \varepsilon - A(\omega)]^2 + B(\omega)^2} \quad (\text{A4})$$

where  $\rho_0(\varepsilon)$  is the bare DOS  $1/(2D) \ln|D/\varepsilon|$ .

This integral can be done by extending the contour to form a semicircle in the upper half plane. The result is approximately

$$\rho_{\text{anal}}(\omega) = \frac{1}{2D} \ln \left( \frac{D}{\sqrt{(\omega - A)^2 + B^2}} \right), \quad (\text{A5})$$

with corrections of order  $B/D^2$ .

<sup>1</sup>C. C. Tsuei *et al.*, Phys. Rev. Lett. **65**, 2724 (1990); D. M. Newns *et al.*, Comments Condens. Matter Phys. **15**, 273 (1992); C. C. Tsuei, C. C. Chi, D. M. Newns, P. C. Pattnaik, and M. Daumling, Phys. Rev. Lett. **69**, 2134 (1992).  
<sup>2</sup>J. Friedel, J. Phys. Condens. Matter **1**, 7757 (1989); J. Labbe and J. Bok, Europhys. Lett. **3**, 1225 (1987).  
<sup>3</sup>R. S. Markiewicz, J. Phys. Condens. Matter **2**, 665 (1990); R. S. Markiewicz, Physica C **200**, 65 (1992).  
<sup>4</sup>P. C. Pattnaik *et al.*, Phys. Rev. B **45**, 5714 (1992); D. M. Newns *et al.*, Phys. Rev. Lett. **73**, 1695 (1994).  
<sup>5</sup>A. A. Abrikosov, J. C. Campuzano, and K. Gofron, Physica C **73**, 214 (1993); K. Gofron *et al.*, Phys. Rev. Lett. **73**, 3302 (1994).  
<sup>6</sup>D. S. Dessau *et al.*, Phys. Rev. Lett. **71**, 2781 (1993); D. M. King *et al.*, *ibid.* **70**, 3159 (1993).  
<sup>7</sup>J. Rossat-Mignod *et al.*, Physica B **186-188**, 1 (1993).  
<sup>8</sup>M. Takigawa, J. L. Smith, and W. L. Hults, Phys. Rev. B **44**, 7764 (1991); M. Takigawa and D. B. Mitzi, Phys. Rev. Lett. **73**, 1287 (1994).  
<sup>9</sup>J. E. Sonier *et al.*, Phys. Rev. Lett. **72**, 744 (1993).

<sup>10</sup>C. C. Tsuei *et al.*, Phys. Rev. Lett. **73**, 593 (1994).  
<sup>11</sup>D. A. Wollman *et al.*, Physica B **194-196**, 1669 (1994).  
<sup>12</sup>R. J. Radtke *et al.*, Phys. Rev. B **48**, 15 957 (1993).  
<sup>13</sup>E. Dagotto *et al.*, Phys. Rev. Lett. **74**, 310 (1995).  
<sup>14</sup>N. Bulut and D. J. Scalapino, Phys. Rev. Lett. **68**, 706 (1992).  
<sup>15</sup>H. Monien, P. Monthoux, and D. Pines, Phys. Rev. B **43**, 275 (1991).  
<sup>16</sup>T. Husslein *et al.* (unpublished).  
<sup>17</sup>H. R. Krishnamurthy *et al.*, Phys. Rev. B **49**, 3520 (1994).  
<sup>18</sup>J. Wheatley and T. Xiang, Solid State Commun. **88**, 593 (1993).  
<sup>19</sup>L. S. Borkowski and P. J. Hirschfeld, Phys. Rev. B **49**, 15 404 (1994).  
<sup>20</sup>J. W. Loram *et al.*, Phys. Rev. Lett. **71**, 1740 (1993).  
<sup>21</sup>A. L. Fetter and J. D. Walecka, *Quantum Theory of Many-Particle Systems* (McGraw-Hill, New York, 1971).  
<sup>22</sup>R. J. Radtke and M. R. Norman, Phys. Rev. B **51**, 3840 (1995).  
<sup>23</sup>K. B. Lyons *et al.*, Phys. Rev. B **37**, 2353 (1988); S. Sugai *et al.*, *ibid.* **38**, 6436 (1988).  
<sup>24</sup>O. K. Andersen *et al.*, Phys. Rev. B **49**, 4145 (1994).